International Journal of Engineering Research
Volume No.4, Issue No.7, pp : 378-383
ISSN:2319-6890)(online),2347-5013(print)
01 July 2015

Dynamic Performance of a Single Machine Brushless DFIG during Wind Speed Variation

Mona N. Eskander, Mahmoud A. Saleh, Maged N. F. Nashed
Electronics Research Institute, Cairo, Egypt
eskander@eri.sci.eg , mahmoudsaleh36@yahoo.com , maged@eri.sci.eg

Abstract: In this paper, the dynamic performance of the specially-designed Single Machine Brushless Doubly-Fed Induction Generator "SM-BDFIG" coupled to variable speed wind turbine is investigated. The rotor voltage of the SM-BDFIG during super-synchronous operation is used to charge a number of batteries, connected to the rotor via a 3-phase bridge rectifier. The number of charged battery cells are changed, by parallel and series connections, according to the wind speed variation, and consequently, the rotor voltage variation. The response of the stator, rotor, and DC link voltages and currents due to wind speed variations is presented. The electromagnetic torque, the stator active power, and the rotor active power during wind speed variations are also presented.

Keywords— Single Machine Brushless Doubly-Fed Induction Generator "SM-BDFIG", 3-phase bridge rectifier, super-synchronous operation, Battery charge, and DC link.

I. Introduction

The recently developed technology in the wind power market, introduces variable- speed working conditions depending on the wind speed in order to optimize the energy captured from the wind. The advantages of variable-speed wind turbines (VSWT) are the 5% greater annual energy capture than the fixed-speed technology, and the easily controlled active and reactive powers [i-iv]. As a disadvantage, VSWT need a power converter that in- creases the system cost. However, if doubly fed induction generator (DFIG) is used with VSWT, the overall cost of the power electronics is reduced because the rating of the converters interfacing the rotor with the grid was proven to be only 10% of the DFIG rating [v].

The benefits of DFIG are undeniable; however, the presence of copper slip rings and carbon brushes to transfer electrical energy to/from the rotating winding of the generator from/to the stationary electronic converter creates the need for frequent inspection and maintenance. Also, the transfer of electric current between the rotating slip rings and the stationary carbon brushes may generate sparks which forbids the WECS installations near explosive environments. The need for frequent maintenance due to the presence of brushes increases sharply the operating costs of WECS especially in remote areas and offshore installations.

To avoid the drawbacks due to brushes, new designs known as brushless double fed induction generators were suggested [vi-ix]. One of these designs proposed two separate induction machines applied in cascade. There were several attempts to develop a 'single-unit' cascade machine in the interests both of reduced cost and improved performance. The most notable of these was due to Hunt [vi].The Hunt motor represented a considerable advance over earlier machines, in that it comprised single stator and rotor windings and a common magnetic circuit. New configurations were developed [vii], where the rotor energy is transferred by using a second fractional induction machine (control machine), which is directly coupled to the main generator (power machine) through the back-to-back connection of rotor circuit. In recent designs, the BDFM is composed of a special rotor and a stator. The stator has two three-phase windings with different pole pair numbers, called power winding (PW) and control winding (CW). Generally, PW is connected directly to the grid and CW is connected to a converter [viii]. The BDFIG has been applied to wind energy conversion systems due to its lower cost and higher reliability [ix].

A new topology of a brushless doubly-fed machine referred to as Rotating Power Electronic Brushless Doubly-Fed Induction Machine (RPE-BDFIM) was developed in [x]. The topology is based on the same control principle as the conventional doubly fed machine. RPE-BDFIM employs two machines; the main machine is the induction machine, which is directly connected to the grid and handles the main portion of the active power while the control machine is a synchronous machine, which handles the slip power. The rotors of the induction and synchronous machines are connected via power electronic converters. However, RPE-BDFIM differs in the way it utilizes the slip power. The existing conventional brushless machine delivers slip power to the grid via the control machine, while in the RPE-BDFIM, slip power is used by the control machine to produce mechanical power which is added to the shaft.

In this paper, dynamic investigation of a new design of a brushless doubly fed induction generator BDFIM that was previously proposed by the authors of this paper [xi] is presented. The new topology of this machine, named single machine- brushless doubly fed induction generator (SM-BDFIG) is composed of three main components; a regular three phase wound rotor induction machine, a power electronic converter, and a pack of rechargeable Lithium-ion batteries. The converter is mounted on the outer surface of a web reinforced hollow metallic (aluminium) or fibber glass cylinder. The battery packs are embedded in the inner part of the cylinder between the webs. The batteries are connected together partly in series and partly in parallel, ending with output terminals carrying the full dc voltage of the whole battery pack. These two terminals are electrically connected to dc terminals of back to back converter. The ac terminals of the converter are connected to the rotor winding of the induction machine. A schematic of the SM-BDFIG is shown in Fig. (1).

ISSN:2319-6890)(online),2347-5013(print)
01 July 2015

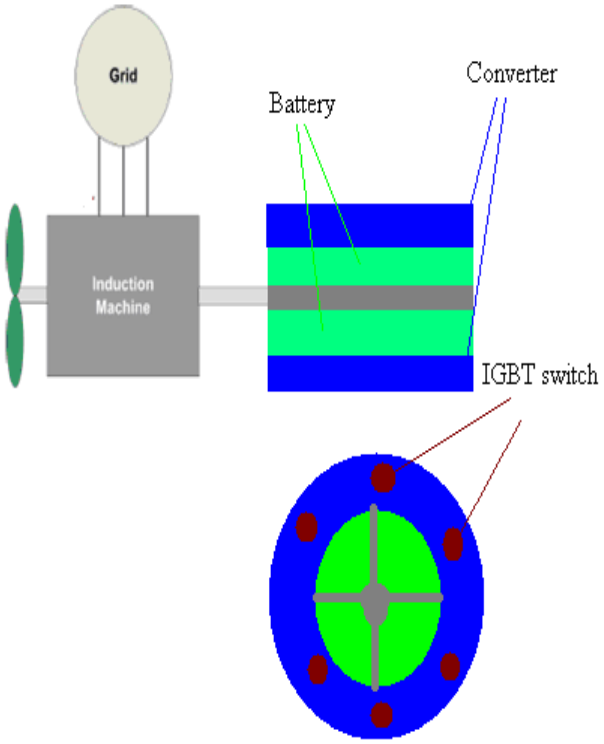

Figure (1) Configuration of SM-BDFIG.

The hollow cylinder is mechanically coupled with the induction machine on the same shaft. Since all the three main components of the SM-BDFIG are mounted on the same shaft, i.e. all rotate with the same angular speed, therefore the connections between them are rigid electrical connections without any sliding contacts, slip rings, or brushes. A detailed description and analysis of the proposed machine merits, parameters, and characteristics was given in the previous research paper [xi].

In this paper, the performance of the SM-BDFIG due to wind speed variation during super synchronous speed is studied. When the SM-BDFIG operates in the super-synchronous speed range, the excess slip power is transferred from the rotor of the induction machine to the converter. This power is converted to dc power, which is used to charge the batteries connected to the rotor via a 3-phase bridge rectifier. The number of charged battery cells are changed, by parallel and series connections, according to the wind speed variation, and consequently, according to the rotor voltage variation. The variations of the stator, rotor, and DC link voltages and currents at two wind speed profiles are presented. The electromagnetic torque, the stator active power, and the rotor active power during wind speed variations are also presented.

II. Modelling SM-BDFIG:

1. DFIG model

The voltage equations for the DFIG in the d-q synchronously rotating axes are given as [iii]:

$$\begin{aligned} v_{sd} &= R_s i_{sd} + \frac{d\lambda_{sd}}{dt} - \omega_s \lambda_{sq} \\ v_{sq} &= R_s i_{sq} + \frac{d\lambda_{sq}}{dt} + \omega_s \lambda_{sd} \\ v_{rd} &= R_r i_{rd} + \frac{d\lambda_{rd}}{dt} - \omega_r \lambda_{rq} \\ v_{rq} &= R_r i_{rq} + \frac{d\lambda_{rq}}{dt} + \omega_r \lambda_{rd} \end{aligned} \quad (1)$$

Where, the stator and rotor magnetic fluxes λ are given by:

$$\begin{aligned} \lambda_{sd} &= (L_{ls} + L_m) i_{sd} + L_m i_{rd} \\ \lambda_{sq} &= (L_{ls} + L_m) i_{sq} + L_m i_{rq} \\ \lambda_{rd} &= (L_{lr} + L_m) i_{rd} + L_m i_{sd} \\ \lambda_{rq} &= (L_{lr} + L_m) i_{rq} + L_m i_{sq} \end{aligned} \quad (2)$$

where R_s, R_r, L_{ls}, and L_{lr} are resistances and leakage inductances for stator and rotor windings respectively;
L_m is the mutual inductance;
v_{sd}, v_{sq},, v_{rd},, v_{rq}, are the d and q components of the stator and rotor voltages respectively
i_{sd}, i_{sq}, i_{rd}, i_{rq}, are the d and q components of the stator and rotor currents respectively
λ_{sd}, λ_{rq}, and λ_{rd}, λ_{rq} are d and q components of stator and rotor magnetic flux respectively
and ω_s and ω_r are angular frequencies of stator and rotor respectively

2. The d-q axis rectifier model

The three-phase diode bridge rectifier, shown in Fig. (2), is connected to the rotor circuit, while its DC output voltage is applied for battery charging.

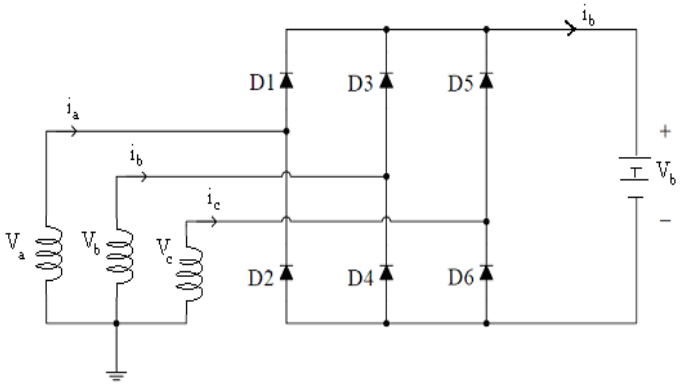

Figure (2) Rectifier Bridge connected to the rotor terminals.

The rectifier is supplied by the balanced three-phase rotor voltage system. Under the balanced conditions, the three-phase sinusoidal voltages at ac side terminals v_a, v_b and v_c can be written as follows:

ISSN:2319-6890)(online),2347-5013(print)
01 July 2015

$$\mathbf{V}_{abc} = \begin{bmatrix} v_a \\ v_b \\ v_c \end{bmatrix} = V_m \begin{bmatrix} \cos(\omega t + \varphi) \\ \cos(\omega t + \varphi - 2\pi/3) \\ \cos(\omega t + \varphi + 2\pi/3) \end{bmatrix} \quad (3)$$

where V_m is the peak rotor voltage magnitude and φ is the initial phase angle. Under this set of voltages, the fundamental of switching functions thus can be expressed as:

$$\mathbf{S}_{abc} = \begin{bmatrix} S_a \\ S_b \\ S_c \end{bmatrix} = \frac{2\sqrt{3}}{\pi} \begin{bmatrix} \cos(\omega t + \varphi) \\ \cos(\omega t + \varphi - 2\pi/3) \\ \cos(\omega t + \varphi + 2\pi/3) \end{bmatrix} \quad (4)$$

The input-output relationships of the diode bridge rectifier are given as:

$$V_{dc} = \mathbf{S}_{abc}^T \mathbf{V}_{abc}$$

$$\mathbf{I}_{abc} = \begin{bmatrix} i_a & i_b & i_c \end{bmatrix}^T = \mathbf{S}_{abc} i_{dc} \quad (5)$$

Consider a synchronously rotating dq frame with d-axis aligned with this voltage vector. Then, the three-phase variables f_{abc} can be expressed in terms of such dq frame using the transformation matrix T such that:

$$\mathbf{f}_{dq} = \mathbf{T} \cdot \mathbf{f}_{abc}$$

and

$$\mathbf{T} = \frac{2}{3} \cdot \begin{bmatrix} \cos\omega t & \cos(\omega t - 2\pi/3) & \cos(\omega t + 2\pi/3) \\ -\sin\omega t & -\sin(\omega t - 2\pi/3) & -\sin(\omega t + 2\pi/3) \end{bmatrix} \quad (6)$$

Hence, the output Dc voltage in terms of the input dq voltages is given as:

$$v_{dc} = \frac{3\sqrt{3}}{\pi} v_{mag} = \frac{3\sqrt{3}}{\pi} \sqrt{v_d^2 + v_q^2}$$

$$i_{mag} = \frac{2\sqrt{3}}{\pi} i_{dc} \quad (7)$$

Where v_{mag} is the magnitude of the voltage vector; v_d and v_q are its d and q axes components, and i_{mag} is the magnitude of the input current with the d and q components as follows:

$$\begin{bmatrix} i_d & i_q \end{bmatrix} = i_{mag} \cdot \begin{bmatrix} \cos\varphi & \sin\varphi \end{bmatrix} \quad (8)$$

Assuming balanced rotor voltage supply, φ can be derived from voltage d- and q components as:

$$\varphi = \tan^{-1}(v_q / v_d) \quad (9)$$

3. Li-Ion Battery Model

The charging equation for a LI-Ion battery is modeled in Matlab software package as:

a- Discharge Model (i* > 0)

$$V_b = E_o + K\frac{Q}{Q - it} i^* - K\frac{Q}{Q - it} it + Ae^{-Bit} \quad (10)$$

b- Charge Model (i* < 0)

$$V_b = E_o - K\frac{Q}{it - 0.1Q} i^* - K\frac{Q}{Q - it} it + Ae^{-Bit} \quad (11)$$

Where,

V_B = Nonlinear voltage (V)
E_0 = Constant voltage (V)
Exp(s) = Exponential zone dynamics (V)
Sel(s) = Represents the battery mode.
Sel(s) = 0 during battery discharge,
Sel(s) = 1 during battery charging.
K = Polarization constant (Ah^{-1}) or Polarization resistance (Ohms)
i* = Low frequency current dynamics (A)
i = Battery current (A)
it = Extracted capacity (Ah)
Q = Maximum battery capacity (Ah)

4. Controller

A PID controller is tuned to allow the SM-BDFIG to follow wind speed variation within a slip ranging from s= 0 (synchronous speed) to s= -0.015. The controller allows maximum power extraction from the wind without exceeding the machine ratings.

III. Simulation and Discussion

The SM-BDFIG system components are modeled in Matlab/Simulink using the above stated equations. The dynamic performance of the system is presented for wind speed with, a step change in wind speed from synchronous to super-synchronous speed.

Figure (3) shows the rotor speed referred to the synchronous speed corresponding to a step change in wind speed. The VSWT is assumed to be operating at synchronous speed, then a step change took place at t=0.25 sec. During the synchronous speed range, two rotor phases are short-circuited and connected to the third rotor phase via a battery supplying the rotor circuit with 30 Volts. This means that the SM-BDFIG operates as a synchronous generator at s=0. Results are given for a 1.5MVA, 690 V, 4 pole induction machine.

The stator active power from synchronous to super synchronous range is given in Fig.(4). It is clear that the step change in wind speed slightly affected the generated stator power. However, as seen from Fig.(5a) presenting the rotor power, a sharp change in the rotor power took place at the step wind speed. The change remained for microseconds only and then power is generated from the rotor side. Figure (5b) zooms the rotor power to clarify the generated power at super synchronous speed.

ISSN:2319-6890)(online),2347-5013(print)
01 July 2015

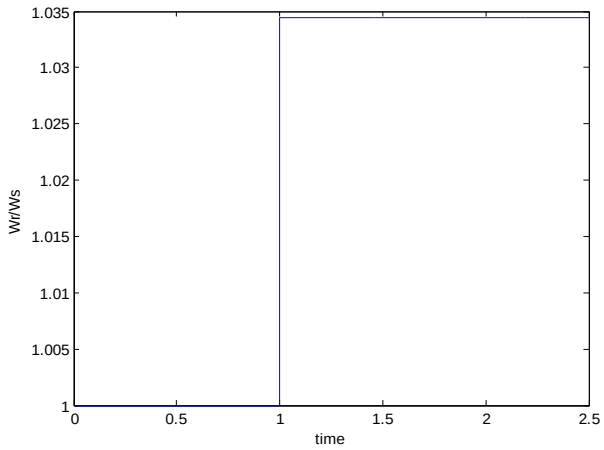

Figure (3) The step change in wind speed.

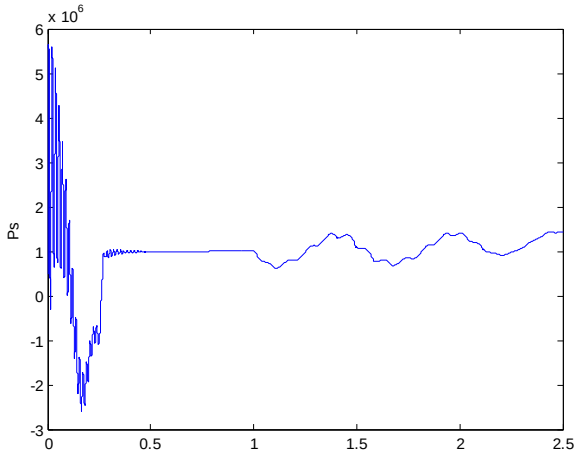

Figure (4) Stator Power.

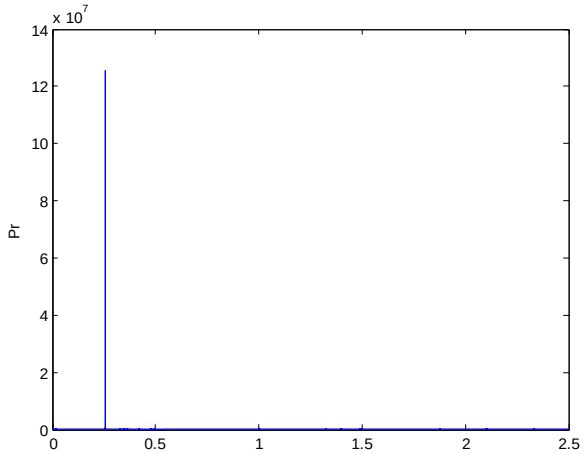

Figure (5a) Rotor Power.

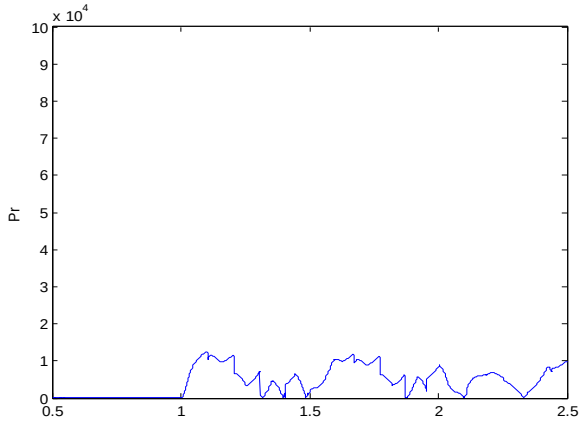

Figure (5b) Zooming the rotor power.

The corresponding rotor current is shown in Fig. (6), showing the sharp short-time change in the current corresponding to wind speed step change. Note that the change in the frequency of rotor current corresponds to the change in super-synchronous speed. Figures (7a) and (7b) show the rotor voltage and its zoom, giving similar performance as rotor current.

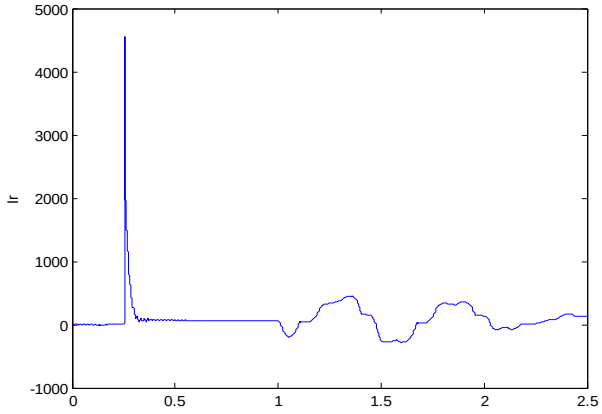

Figure (6) Rotor current.

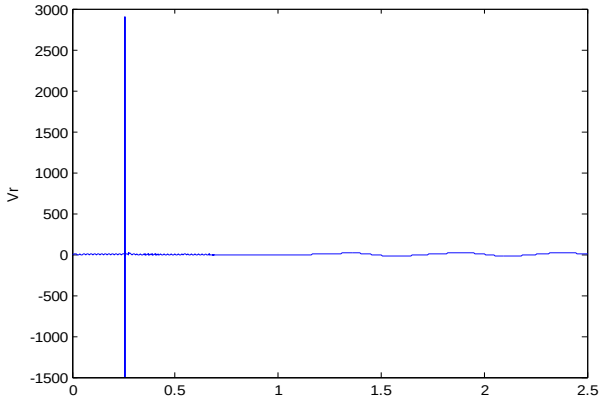

Figure (7a) Rotor Voltage

ISSN:2319-6890)(online),2347-5013(print)
01 July 2015

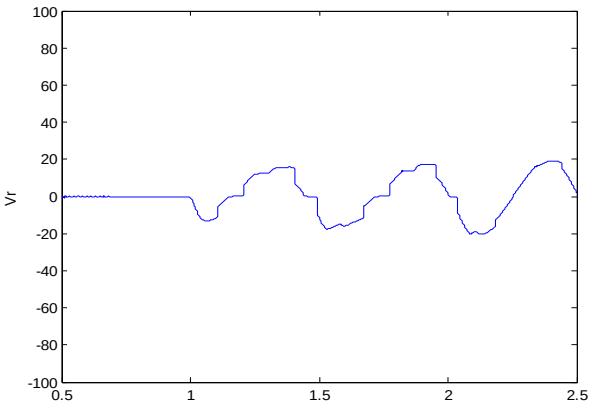

Figure (7b) Zooming Rotor Voltage.

Figure (8) presents the dc voltage output from the rectifier and used to charge the batteries. The sharp change lasts for very short time, so it is harmless to the battery bank. Figure (9) presents the dc current, showing a fast damping spike due to the step change in wind speed.

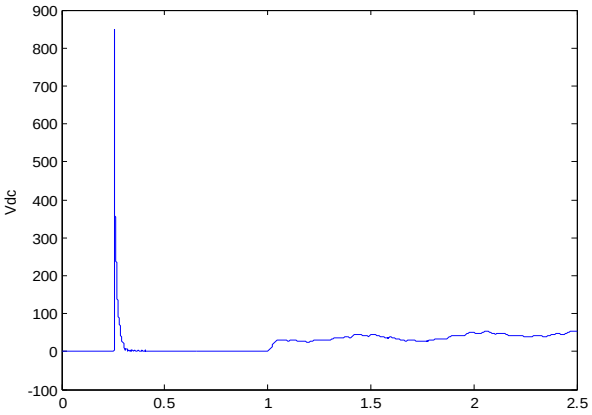

Figure (8) DC Rectifier Voltage.

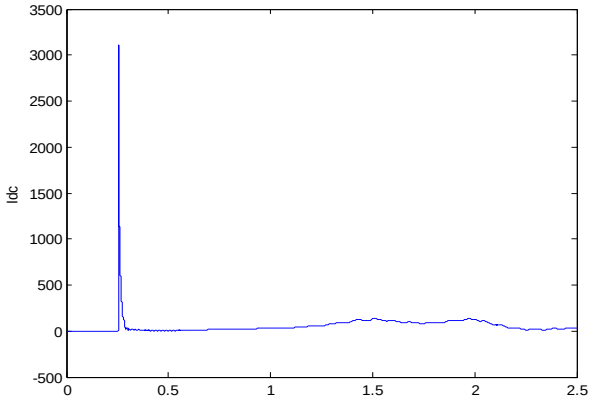

Figure (9) The dc link current.

The electromagnetic torque, shown in Fig. (10), suffers also from this step function but reaches steady state within short interval

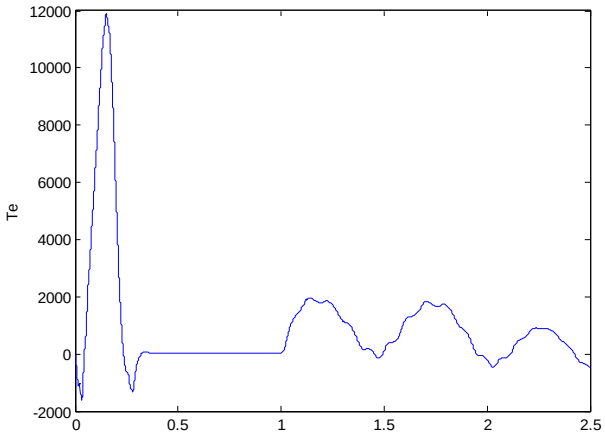

Figure (10) Electromagnetic Torque.

IV. Conclusion

The dynamic performance of the specially-designed Single Brushless Doubly-Fed Induction Generator "SM-BDFIG" coupled to variable speed wind turbine is investigated. The rotor voltage of the SM-BDFIG during super-synchronous operation is used to charge a number of batteries, connected to the rotor via a 3-phase bridge rectifier. A PID controller is designed and tuned to allow the SM-BDFIG to follow the wind speed leading to maximum power tracking. The proposed generator, the controller, the rectifier, and the battery pack are modelled. A step change in the wind speed is assumed and the response of the stator, rotor, dc bridge voltage and dc current are investigated through simulation using Matlab/Simulink software. The Results showed that the stator parameters were slightly affected by the wind speed variation, while rotor parameters are sharply affected. However, recovery to steady state values was quick, which proves safe performance of the proposed generator components.

Future work will investigate methods of decreasing peaks in rotor currents and voltages for more reliable performance.

Appendix

Rated Power: 1.5 MVA,
Voltage : 690 Volt, 60 Hz,
No. of Poles : 4,
Stator Resistance : 1.4 m Ω,
Stator Inductance : 90 μ H,
Rotor Resistance : 0.99 m Ω,
Rotor Inductance : 82.1 μ H,
Mutual Inductance : 1.526 m H,
Moment of inertia : 18.7 Kg.m^2

ISSN:2319-6890)(online),2347-5013(print)
01 July 2015

REFERENCES

i. *Hyong Sik Kim, and Dylan Dah-Chuan Lu, "Wind Energy Conversion System from Electrical Perspective -A Survey", Smart Grid and Renewable Energy, 2010, vol. 1, pp.119-131.*

ii. Gonzalo Abad, Jesu´s Lo´pez, Miguel A. Rodrı´guez, and Luis Marroyo Grzegorz Iwanski, "Doubly Fed Induction Machine-Modeling And Control For Wind Energy Generation", Published by John Wiley & Sons, Inc., Hoboken, New Jersey, 2011.

iii. Bin Zhao, Hui Li, Mingyu Wang, Yaojun Chen, Shengquan Liu, Dong Yang, Chao Yang, Yaogang Hu, and Zhe Chen, "An Optimal Reactive Power Control Strategy for a DFIG-Based Wind Farm to Damp the Sub-Synchronous Oscillation of aPower System" Energies 2014, 7, 3086-3103; doi:10.3390/en7053086, ISSN 1996-1073, www.mdpi.com/journal/energies

iv. Mahmoud A. Saleh, Maged N. F. Nashed, and Mona N. Eskander, "An Approach to Determine the Impact of Wind Speed Variations on the Output Power of Wind-Driven DFIG", Journal of Next Generation Information Technology (ISSN: 2092-8637), Vol.3, No.1, Feb. 2012, pp7-17.

v. Mahmoud Abdel Halim Saleh, and Mona Naguib Eskander, "Sizing of Converters Interfacing the Rotor of Wind Driven DFIG to the Power Grid", Smart Grid and Renewable Energy, 2011, 2, 300-304, Published Online August 2011 (http://www.SciRP.org/journal/sgre)

vi. Hunt, L. J., 'A new type of induction motor', IEE, 1907, 39, pp. 648-667.

vii. Kostyantyn Protsenko and Dewei Xu, "Modeling and Control of Brushless Doubly-Fed Induction Generators in Wind Energy Applications", IEEE Transactions On Power Electronics, Vol. 23, No. 3, MAY 2008.

viii. Ai-ling Zhang, and Xin Wang, "A Static Two-Axis Model and Its Application in Direct Torque Control System for Brushless Doubly Fed Induction Machine", IEEE PEDS 2011, Singapore, 5–8 December 2011, pp: 968-973.

ix. Teng Long, Shiyi Shao, Ehsan Abdi, Richard A. McMahon, and Shi Liu, "Asymmetrical Low-Voltage Ride Through of Brushless Doubly Fed Induction Generators for the Wind Power Generation", IEEE Transactions On Energy Conversion, Vol. 28, No. 3, September 2013.

x. Naveedur Rehman Malik, and Chandur Sadarangani, "Brushless Doubly-fed Induction Machine with Rotating Power Electronic Converter for Wind Power Applications", International conference on Electrical Machines and Systems (ICEMS), 2011, Beijing, 20-23 Aug. 2011

xi. Mahmoud A. Saleh and Mona N. Eskander, "A Single Machine Brushless DFIG for Grid-Connected and Stand-Alone WECS" British Journal of Applied Science & Technology 4 (24): 3550-3562, 2014, SCIENCEDOMAIN international, www.sciencedomain.org.